

## Global Control of Spiral Wave Dynamics in an Excitable Domain of Circular and Elliptical Shape

V. S. Zykov, G. Bordiougov, H. Brandtstädter, I. Gerdes, and H. Engel

*Institut für Theoretische Physik, Technische Universität Berlin, Hardenbergstrasse 36, D-10623 Berlin, Germany*

(Received 22 August 2003; revised manuscript received 11 November 2003; published 9 January 2004)

Experiments performed in a thin layer of the Belousov-Zhabotinsky solution subjected to a global feedback demonstrate the existence of the resonance attractor for meandering spiral waves within a domain of circular shape. In an elliptical domain, the resonance attractor can be destroyed due to a saddle-node bifurcation induced by a variation of the domain eccentricity. This conclusion explains the experimentally observed anchoring of spiral waves at certain points of an elliptical domain and is in good quantitative agreement with numerical data obtained for the Oregonator model.

DOI: 10.1103/PhysRevLett.92.018304

PACS numbers: 82.40.Bj, 05.45.Gg, 05.65.+b, 47.54.+r

Recent experiments demonstrate that reaction-diffusion systems subjected to a global feedback control can exhibit very rich spatiotemporal dynamics [1–3]. In particular, a spiral wave (generic pattern in excitable media) can be effectively manipulated applying global feedback [3,4]. This opportunity is important for various applications, e.g., for the low voltage defibrillation of cardiac tissue [5]. It was shown recently that the size of the excitable domain is a very essential control parameter affecting the stability of the rigidly rotating spiral or changing the radius of the resonance attractor (motion of the spiral wave core along a closed circular orbit) [6,7]. These findings allow one to assume that the shape of the excitable domain can also have a great impact on the dynamics of spiral waves.

We report in this Letter experimental results for the evolution of meandering spiral waves in circular and elliptic domains under global feedback focusing on the effect of the domain shape on their dynamics. Then we present a theoretical approach that allows one to determine the velocity field of the resonant drift induced by the global feedback. Finally, the predictions of this approach are compared to numerical data obtained for the underlying reaction-diffusion model.

The experiments were performed with the light-sensitive version of the Belousov-Zhabotinsky (BZ) reaction by the use of an open reactor [8]. A premixed feeding solution prepared from stock solutions containing  $[\text{NaBrO}_3]_0 = 2.06 \times 10^{-1} \text{ M}$  (Aldrich, 99%),  $[\text{H}_2\text{SO}_4]_0 = 30.1 \times 10^{-1} \text{ M}$  (Aldrich, 95%–98%), malonic acid (MA)  $[\text{CH}_2(\text{COOH})_2]_0 = 1.86 \times 10^{-1} \text{ M}$  (Aldrich, 99%), and  $[\text{NaBr}]_0 = 4.12 \times 10^{-2} \text{ M}$  (Fluka, 99%) is pumped continuously through the reactor with the rate 120 ml/h. Circulating water from a thermostat maintains the temperature at  $25.0 \pm 0.5 \text{ }^\circ\text{C}$ . The catalyst is immobilized in a silicahydrogel layer of 0.5 mm thickness (active layer) prepared on a plate of frozen glass (diameter 63 mm). To protect the active layer from stirring effects, it is covered by an inactive gel layer not loaded with the catalyst.

The active layer is illuminated by a video projector (Panasonic PT-L555E) controlled by a computer via a frame grabber (Data Translation, DT 2851). The illuminating light is filtered with a bandpass filter (BG6, 310–530 nm). Every second, the pictures of the oxidation waves appearing in the gel layer are detected in transmitted light by a charge-coupled device camera (Sony AVC D7CE) and digitized with a frame grabber (Data Translation, DT 3155) for immediate processing by the computer. During the same time step, the signal controlling the projector can be changed in accordance with the processed information to close the feedback loop.

A single spiral wave is created in the gel disk by breaking a wave front with a cold intense light spot. The location of the spiral wave tip is defined on-line as the intersection point of contour lines ( $0.6 \times$  amplitude) extracted from two digitized images taken with time interval 2.0 s. The tip trajectory can be visualized during the experiment by the computer.

An unperturbed spiral has a wavelength  $\lambda \approx 2.0 \text{ mm}$ . Its tip describes a meandering trajectory containing about four lobes. The rotation period measured far away from the symmetry center is  $T_\infty \approx 40 \text{ s}$ .

To realize a global feedback, the illumination intensity  $I(t)$  is computed as

$$I(t) = I_0 + k_{fb}[B(t - \tau) - B_0], \quad (1)$$

where  $B(t)$  specifies an image gray level  $g(x, y, t)$  averaged over the integration area  $S$ :

$$B(t) = \frac{1}{S} \int_S g(x, y, t) dx dy. \quad (2)$$

The area  $S$  represents a virtual excitable domain as illustrated in Fig. 1. Constants  $I_0$  and  $k_{fb}$  and  $\tau$  in (1) determine the background intensity, the gain, and the time delay in the feedback loop. Constant  $B_0$  specifies the integral  $B(t)$  computed for a spiral wave rotating around the center of a circular domain.

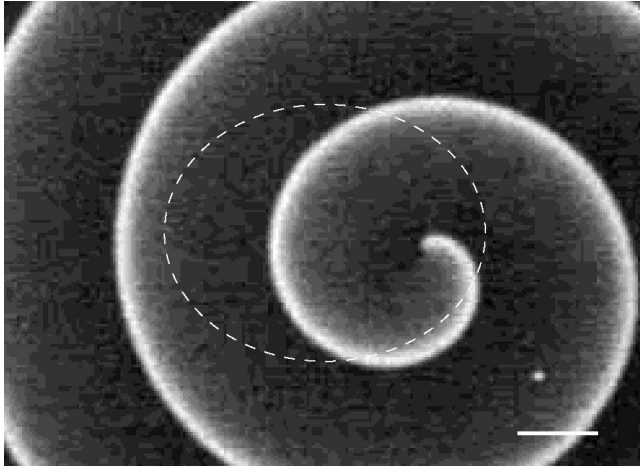


FIG. 1. Snapshot of a spiral wave rotating in a thin layer of the BZ reaction. The dashed line indicates the boundary of an elliptical integration area  $S$ . Scale bar: 1 mm.

Figures 2(a)–2(c) show spiral tip trajectories of the feedback induced drift observed in a circular domain for different time delays  $\tau$  in the feedback loop. While for  $\tau = 0$  the trajectory of the spiral center reaches a circular orbit of radius  $R_a \approx 0.65\lambda$ , for  $\tau/T_\infty = 0.32$  the attractor radius decreases to  $R_a = 0.45\lambda$  [see Fig. 2(b)]. For  $\tau = 0.5T_\infty$ , the spiral core center tends towards the domain center that corresponds to  $R_a = 0$ . Figure 3 summarizes the experimental results for the

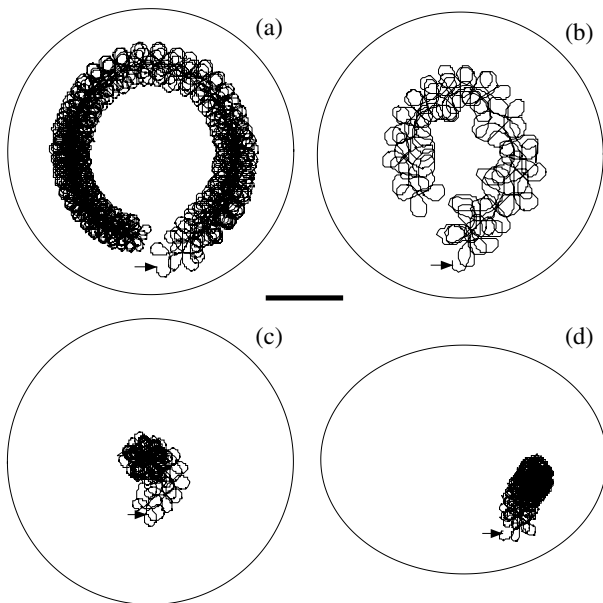


FIG. 2. Resonant drift of a spiral wave induced by a global feedback with  $k_{fb} = -1.5$ ,  $B_0 = 25$ , and  $I_0 = 70$ . (a)–(c) Circular domain of radius  $R = \lambda$ ; (d) elliptical domain with large axis  $a = 2\lambda = 4$  mm and small axis  $b = a/1.25$ . In (a) and (d), the time delay is  $\tau = 0$ , in (b)  $\tau/T_\infty = 0.32$ , and in (c)  $\tau/T_\infty = 0.5$ . Initial spiral tip locations are marked by arrows. Scale bar: 1 mm.

radius  $R_a$  of the resonance attractor as a function of the time delay  $\tau$  in the feedback loop.

Figure 2(d) demonstrates a qualitatively different drift trajectory observed in an elliptical domain. After a transient process, the drift velocity vanishes and the spiral waves rotate around some point located at a distance of about  $0.6\lambda$  from the domain center.

In order to explain these experimental findings, note that the reason for the resonant drift is a periodic modulation of the illumination intensity  $I(t)$  [9–11], induced by variations of the integral  $B(t)$  [see Eq. (1)]. If the spiral wave core moves rather slow, the integral  $B(t)$  oscillates with the rotation period  $T_\infty$  of the spiral wave. Only the first component in the Fourier series of the periodic modulation causes a resonant drift [12,13]. This first component can be written as  $A \cos(\omega t - \phi)$ , where  $\omega = 2\pi/T_\infty$  and the amplitude  $A$  and the phase  $\phi$  depend on the location of the spiral core center. These dependencies can be found rather easily under assumption that far away from the core center a rotating wave front can be approximated by an Archimedean spiral

$$\Theta(r, t) = \Theta_0 - \frac{2\pi}{\lambda} r + \omega t, \quad (3)$$

where  $(\Theta, r)$  are polar coordinates with origin at the core center. The integral  $B(t)$  should be proportional to the arclength  $L$  of the spiral wave front within the integration domain, since an excitation wave in the BZ solution looks like a rather thin stripe [7].

These assumptions allow one to reduce the estimation of the amplitude  $A(x, y)$  and the phase  $\phi(x, y)$  to a pure geometrical procedure. We imagine that the center of an Archimedean spiral described by Eq. (3) with  $\Theta_0 = 0$  is placed at a point  $(x, y)$ . Then the arclength  $L$  of the spiral within a domain of a given shape will be a periodic function of time and the first Fourier component of this function gives us the amplitude  $A(x, y)$  and the phase  $\phi(x, y)$  of the integral  $B(t)$ . The modulation amplitude

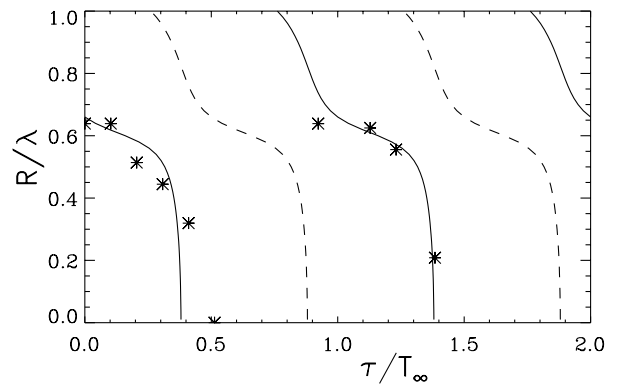


FIG. 3. The radius  $R_a$  of the resonance attractor (asterisks) as a function of the time delay  $\tau$  observed experimentally in a circular domain of radius  $R_d = \lambda$ . Solid curves and dashed curves represent radii of the resonance attractors and the unstable orbits obtained from Eq. (6) with  $\varphi = -0.82$ .

of  $I(t)$  will be proportional to  $A(x, y)$  due to Eq. (1) and the modulation phase will be shifted by  $\omega\tau$  with respect to  $\phi(x, y)$ .

If the induced drift is so slow that the shape and the angular velocity of the rotating spiral remain always the same, the absolute value of the core velocity  $V(x, y)$  is proportional to the amplitude  $A(x, y)$  and the drift direction is specified by an angle

$$\gamma = \varphi + \omega\tau + \phi(x, y). \quad (4)$$

Here  $\varphi$  is a constant that specifies the direction of the drift induced in the case  $\tau = 0$  and  $\phi = 0$ . Then the motion of the core center can be described as a system of two ordinary differential equations:

$$\frac{dx}{dt} = V(A) \cos\gamma, \quad \frac{dy}{dt} = V(A) \sin\gamma. \quad (5)$$

Figure 4(a) shows the drift velocity field obtained by application of the described procedure for a circular shape of an excitable domain of radius  $R_d = \lambda$  with zero time delay  $\tau = 0$  and  $\varphi = -0.5$ . The drift velocity  $V(x, y)$  vanishes at the domain center representing an unstable node. This node is surrounded by a stable limit cycle, at which the drift velocity is constant  $V(x, y) = V_c$  and orthogonal to the radial direction. This limit cycle represents the resonance attractor of spiral waves [7].

Because of the rotational symmetry of the circular domain and in accordance with Eq. (4), the drift will be orthogonal to a radial displacement  $R$  only when

$$\omega\tau + \phi(R) = 0.5\pi - \varphi + 2\pi n. \quad (6)$$

This condition determines the radius  $R$  of a circular orbit as a function of the time delay. The orbit is stable if  $n = 2m$  [7]. The radius  $R_a$  of the resonance attractor computed from Eq. (6) as a function of the time delay is shown in Fig. 3 by solid lines. It predicts rather well the experimental data shown by asterisks. Dashed curves in Fig. 3 specify radii of unstable orbits with  $n = 2m + 1$  separating basins of attraction.

Figure 4(b) shows the velocity field corresponding to a domain of elliptical shape. The large ellipse axis  $a$  is equal to  $2\lambda$  and its ratio to the small axis  $b$  is equal to  $a/b = 1.25$ . The deviation with respect to a circular shape drastically changes the velocity field plotted in Fig. 4(a). While in a circular domain the drift velocity along the resonance attractor is constant, a deviation from the circular shape induces variations of the drift velocity along the orbit. At some segments the drift becomes faster, at other slower than in the circular domain. A closer inspection reveals that, when the eccentricity of an elliptical domain is large enough, the tangent component of the drift velocity vanishes at two diametrically opposite saddle-node points where  $A(x, y) = 0$ . Beyond the bifurcation, for eccentricity larger than the critical value, saddles and stable nodes separate from each other and two pairs of fix points emerge, as shown in Fig. 4(b).

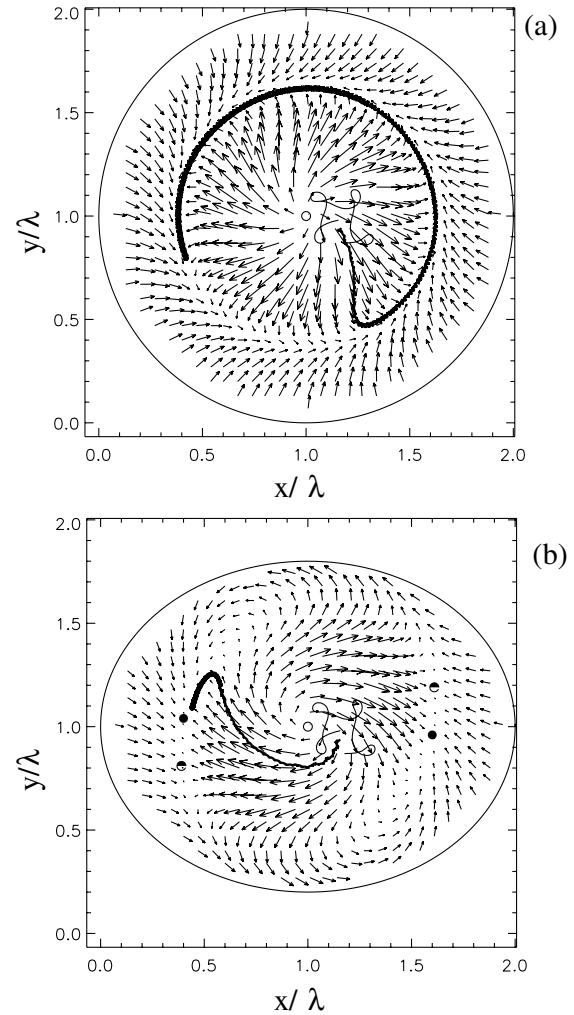


FIG. 4. Velocity field of the spiral core drift induced by the global feedback computed in the approximation of an Archimedean spiral for (a) a circular and (b) an elliptical domain with  $a/b = 1.25$ . Open (filled) circles indicate unstable (stable) nodes. Semifilled circles show saddles. Initial four lobes of the tip trajectories (thin solids) and the trajectories of a core center (thick solids) computed from the reaction-diffusion model (7) are shown.

This bifurcation destroys the former limit cycle corresponding to the resonance attractor. Depending on the initial conditions, asymptotically the spiral wave can approach one of two stable nodes and remains anchored at this point at a distance of about  $0.6\lambda$  from the domain center.

The results of this theoretical consideration are compared with the numerical data obtained by integration of the Oregonator model of the BZ reaction:

$$\begin{aligned} \frac{\partial u}{\partial t} &= \nabla^2 u + \frac{1}{\epsilon} \left[ u - u^2 - (fv + I) \frac{u - q}{u + q} \right], \\ \frac{\partial v}{\partial t} &= u - v. \end{aligned} \quad (7)$$

Here the variables  $u$  and  $v$  correspond to the concentrations of the autocatalytic species  $\text{HBrO}_2$  and the oxidized

form of the catalyst, respectively. The parameters  $\epsilon = 0.05$ ,  $q = 0.002$ , and  $f = 2.0$  were fixed. The term  $I = I(t)$  describes the bromide production that is induced by the external illumination [14]. The computations were performed by the explicit Euler method on a  $380 \times 380$  array with a grid spacing  $\Delta x = 0.2$  and time steps  $\Delta t = 0.002$ . In order to simulate a global feedback,  $I(t)$  is determined by Eqs. (1) and (2) with  $g(x, y, t) = v(x, y, t)$ ,  $I_0 = 0.01$ ,  $k_{fb} = -0.1$ , and  $B_0 = 0.06$ .

The trajectory of the core center computed from the reaction-diffusion system (7) in a circular domain is shown in Fig. 4(a) by a thick solid curve. The location of the final circular orbit and the whole transient process correspond very well to the determined drift velocity field. The trajectory obtained for the same initial core location in an elliptical domain is shown in Fig. 4(b). In this case, the spiral core after a transient process remains to be anchored near one of the stable nodes of the predicted velocity field.

Thus, the performed experimental study provides the very first observation of the resonance attractor for a meandering spiral wave subjected to a global feedback. The radius of the attractor orbit can be effectively manipulated by varying of the time delay in the feedback loop. It is found also that the shape of the excitation domain plays an extremely important role for the dynamics of spiral waves under global feedback control. In particular, a relatively small deformation of the domain shape can destroy the resonance attractor and create separate attracting points [see Fig. 2(d)].

The theoretical approach developed in [7] for the analysis of spiral wave dynamics under weak feedback control is generalized here in two ways: It is expanded to the domains of arbitrary shape, and it is extended to the case of a meandering spiral waves. For a circular domain, this approach predicts the dependence of the resonance attractor radius on the time delay in the feedback loop in good agreement with the experimental results (see Fig. 3). For an elliptical domain, it allows one to explain the experimentally observed anchoring of the spiral wave at certain points in the medium. The predicted locations of the new nodes are in perfect agreement with numerical integrations of the Oregonator model (see Fig. 4) and with the experimental data shown in Fig. 2(d).

The proposed approach is based on two common assumptions: (i) The spiral wave has an Archimedean shape (e.g., see [15,16]) and (ii) the drift velocity is slow. Hence, the obtained results can be applied to media with quite different local kinetics. While the light-sensitive BZ reaction is the most convenient object for an experimental investigation of feedback controlled excitable systems, spiral waves are intensively studied in the context of catalytic surface reactions [2] and excitation waves in cardiac tissue [17] also. In the last case, the spatiotemporal evolution of the fast variable  $u$  (transmembrane po-

tential) rather than slow variable  $v$  (oxidized form of the catalyst in the BZ reaction) is measured. This, however, does not influence the main results reported in this Letter, because to plot the drift velocity field one needs to determine such characteristics of a spiral wave ( $\lambda$ ,  $\omega$ ,  $\varphi$ ), which do not depend on what kind of variable is recorded.

In conclusion, besides the domain size, the time delay  $\tau$ , and the gain  $k_{fb}$  in the feedback loop, the shape of the excitable domain proved to be another essential control parameter for spiral wave dynamics under global feedback. We reveal in this Letter bifurcations in the velocity field of resonant drift induced by variation of the domain shape, which are connected with dramatic changes in the dynamics of the spiral wave. The study of corresponding bifurcations under combined variations of the domain shape, size, and/or the time delay in the feedback loop is an interesting challenge from the theoretical point of view and an important task for various practical applications.

The authors thank the Deutsche Forschungsgemeinschaft (DFG, SFB 555) for financial support.

- 
- [1] V. K. Vanag, L. Yang, M. Dolnik, A. M. Zhabotinsky, and I. Epstein, *Nature (London)* **406**, 389 (2000).
  - [2] M. Kim, M. Bertram, M. Pollman, A. von Oertzen, A. S. Mikhailov, H. H. Rotermund, and G. Ertl, *Science* **292**, 1357 (2001).
  - [3] O. U. Kheowan, C. K. Chan, V. S. Zykov, O. Rangsiman, and S. C. Müller, *Phys. Rev. E* **64**, 035201(R) (2001).
  - [4] V. S. Zykov, A. S. Mikhailov, and S. C. Müller, *Phys. Rev. Lett.* **78**, 3398 (1997).
  - [5] A. V. Panfilov, S. C. Müller, V. S. Zykov, and J. P. Keener, *Phys. Rev. E* **61**, 4644 (2000).
  - [6] O. Kheowan, V. S. Zykov, and S. C. Müller, *Phys. Chem. Chem. Phys.* **4**, 1334 (2002).
  - [7] V. S. Zykov and H. Engel, *Phys. Rev. E* **66**, 16206 (2002).
  - [8] M. Braune and H. Engel, *Phys. Rev. E* **62**, 5986 (2000).
  - [9] K. I. Agladze, V. A. Davydov, and A. S. Mikhailov, *JETP Lett.* **45**, 767 (1987).
  - [10] M. Braune, A. Schrader, and H. Engel, *Chem. Phys. Lett.* **222**, 358 (1994).
  - [11] S. Grill, V. S. Zykov, and S. C. Müller, *J. Phys. Chem.* **100**, 19 082 (1996).
  - [12] V. A. Davydov, V. S. Zykov, and A. S. Mikhailov, *Usp. Fiz. Nauk* **161**, 45 (1991) [*Sov. Phys. Usp.* **34**, 665 (1991)].
  - [13] R. M. Mantel and D. Barkley, *Phys. Rev. E* **54**, 4791 (1996).
  - [14] H.-J. Krug, L. Pohlmann, and L. Kuhnert, *J. Phys. Chem.* **94**, 4862 (1990).
  - [15] N. Wiener and A. Rosenblueth, *Arch. Instit. Cardiol. Mex.* **16**, 205 (1946).
  - [16] A. T. Winfree, *Science* **175**, 634 (1972)
  - [17] J. M. Davidenko, A. V. Pertsov, R. Salomonsz, W. Baxter, and J. Jalife, *Nature (London)* **355**, 349 (1992).